RESEARCH ARTICLE

Using Plant Proteins to Develop Composite Scaffolds for Cell Culture Applications

Linzhi Jing[1,2], Jie Sun[3]*, Hang Liu[1,2], Xiang Wang[1,2], Dejian Huang[1,2]*

[1]National University of Singapore (Suzhou) Research Institute, Suzhou, Jiangsu 215123, China
[2]Department of Food Science and Technology, National University of Singapore, Singapore 117543, Singapore
[3]Department of Mechatronics and Robotics, Xi'an Jiaotong-Liverpool University, Suzhou, Jiangsu 215123, China

Abstract: Electrohydrodynamic printing (EHDP) is capable of fabricating scaffolds that consist of micro/nano scale orientated fibers for three-dimensional (3D) cell culture models and drug screening applications. One of the major hurdles that limit the widespread application of EHDP is the lack of diverse biomaterial inks with appropriate printability and desired mechanical and biological properties. In this work, we blended plant proteins with synthetic biopolymer poly(ε-caprolactone) (PCL) to develop composite biomaterial inks, such as PCL/gliadin and PCL/zein for scaffold fabrication through EHDP. The tensile test results showed that the composite materials with a relatively small amount of plant protein portions, such as PCL/gliadin-10 and PCL/zein-10, can significantly improve tensile properties of the fabricated scaffolds such as Young's modulus and yield stress. These scaffolds were further evaluated by culturing mouse embryonic fibroblasts (NIH/3T3) cells and proven to enhance cell adhesion and proliferation, apart from temporary inhibition effects for PCL/gliadin-20 scaffold at the initial growth stage. After these plant protein nanoparticles were gradually released into culture medium, the generated nanoporous structures on the scaffold fiber surfaces became favorable for cellular attachment, migration, and proliferation. As competent candidates that regulate cell behaviors in 3D microenvironment, such composite scaffolds manifest a great potential in drug screening and 3D *in vitro* model development.

Keywords: Composite biomaterials ink; Electrohydrodynamics; Additive manufacturing

***Correspondence to:** Jie Sun, Mechatronics and Robotics, Xi'an Jiaotong-Liverpool University, Suzhou, Jiangsu 215123, China; jie.sun@xjtlu.edu.cn. Dejian Huang, Department of Food Science and Technology, National University of Singapore, Singapore 117543, Singapore; fsthdj@nus.edu.sg

Received: June 16, 2020; **Accepted:** September 11, 2020; **Published Online:** October 30, 2020

Citation: Jing L, Sun J, Liu H, *et al*., 2021, Using Plant Proteins to Develop Composite Scaffolds for Cell Culture Applications. *Int J Bioprint,* 7(1):298. http://doi.org/10.18063/ijb.v7i1.298

1. Introduction

Three-dimensional (3D) scaffolds have been developed to facilitate cell culture to circulate nutrition and remove metabolic waste[1]. Such scaffolds have drawn an intensive attention in the fields of cell biology, tissue engineering, and drug discovery since the produced 3D *in vitro* models can closely mimic the cellular states in physiological environment and enhance cell migration, proliferation, and functionalities[2]. For example, 3D collagen gel structure can support fibroblasts to elongate themselves to spindle shape, migrate, and invade similar to *in vivo* observation, whereas they developed prominent stress fibers and became immobile in 2D glass substrate[3]. A 3D reconstituted basement membrane can prompt mammary epithelial cells to self-assemble into spherical structures with a central lumen approximating to normal mammary acini[4]. The metabolic rates of human breast cancer grown on the 3D chitosan scaffold approximated to those *in vivo* tumors[5]. In 3D cell culture, scaffolds' physical and chemical properties can significantly influence cell adhesion, migration, and differentiation. These properties can be detected by the adhesion proteins on the cell membrane and transmitted into downstream biochemical signals[6]. Thus, understanding cell-scaffold interaction is crucial for understanding fundamental cellular behaviors and designing new biomaterial inks.

Traditional scaffolding methods such as freeze-drying, gas-forming, and solvent-casting particulate leaching can produce sponge structure scaffolds for cell culture, but they are not capable of controlling scaffolds' microstructure, which is critical for cell-scaffold interactions[7]. Recent advances in 3D printing, also known as additive manufacturing, bring new chances to fabricate scaffolds with customizable microstructures in reproducible features[8]. For instance, extrusion-based 3D printing such as fused deposition modeling has been widely used to fabricate polymer-based fibrous scaffolds for biomedical devices[9]. Droplet-based bioprinting enables precise control on deposition of microdroplets containing biological substances, such as growth factors, cells, modified genes, small molecule drugs, and biomaterials, in a fast and high-resolution manner. Vat polymerization-based bioprinting allows direct fabrication of high-resolution cell-laden tissue constructs[10].

Among these 3D printing methods, electrohydrodynamic printing (EHDP) has drawn great interest for its capability of producing ultrafine fibers with high resolution and reproducibility[11]. Like the working principle of near-field electrospinning, EHDP employs a high electric field to induce fiber ejection from viscous biopolymer solution, ranging from a few hundreds of nanometers to micrometers, from viscous biopolymer solution.[12]. However, very limited polymer materials are available for this technique due to the harsh requirement on biomaterial ink properties.

The scaffold materials should provide temporary support for cells to attach, proliferate, and deliver bioactive components. In general, synthetic biopolymers such as polyethylene glycol, poly(vinyl alcohol), poly(lactide-co-glycolide), and poly-ε-caprolactone (PCL) are usually used as scaffold materials due to their excellent printability, favorable biodegradability, and biocompatibility[13]. They can be applied to common scaffold fabrication methods to produce porous scaffolds with varied pore size, shape, interconnectivity, and porosity[14]. Especially, PCL, a biodegradable polyester with a low melting point, has received extensive attention on accounts of its ideal rheological and viscoelastic properties, excellent solubility, and biocompatibility[15]. However, the *in vivo* degradation period of PCL is up to few years due to its hydrophobicity and semi-crystallinity[16]. A simple way to overcome this bottleneck is to prepare composite materials by mixing PCL with hydrophilic polymers extracted from animals such as collagen and alginate. The properties of these natural derived components may vary from batch to batch and bring in safety concern like transmission of zoonotic diseases.

Compared with animal-derived components, plant proteins, such as zein and gliadin, are favorable choices due to their wide availability, consistent quality, and structural diversity[17]. As alcohol-soluble plant proteins, zein protein contains different subunits including α-zein (75 – 85 wt% of zein), β-zein, γ-zein, and δ-zein with different molecular weight and composition. Similarly, gliadin also consists of various fractions. Both zein and gliadin can be fabricated into various structures such as thin films, nanoparticles, fibers, and porous scaffold. The poor mechanical strength of natural polymers can be improved by mixing with synthetic polymers. As a class of prolamin protein found in corn, zein resists to microbial attacks and has been applied as coating material for encapsulated nutrition and drugs[18]. Zein has been regarded as a potential biopolymer candidate with its hydrophobicity, cytoaffinity, and biodegradability[19]. Porous zein scaffold can support rat mesenchymal stem cells to grow and differentiate into osteoblasts *in vitro*[16]. Because of the amphiphilic and biodegradable nature of zein, researchers mixed zein with synthetic polymers and produced PCL/zein fibers by coaxial electrospinning to release metronidazole in a controlled manner[20]. Thus, blending PCL with zein to prepare composite biomaterial inks may be an effective way to improve scaffolds' cell affinity and biodegradability.

Gliadin, one of the major gluten storage proteins of wheat, has been investigated for its carrier role for controlled release of lipophilic and cationic drugs due to its unique physicochemical properties[21]. It can also deliver sensitive enzymes and avoid their breakdown by stomach acids. Nevertheless, further developments of gliadin are hindered by its low water stability and immunogenic toxicity in patients with celiac disease[22]. An alternative plan is to blend a small amount of gliadin with PCL in the preparation of composite biomaterial inks for scaffold fabrication, with the purpose of improving cell affinity and suppressing gliadin's side effect. In short, both zein and gliadin are abundant and structurally diverse, which may overcome the current limitations of components extracted from animals in terms of their supply and quality. These plant proteins are also easy to blend with other synthetic biopolymers because of their specific solubility and film-forming properties.

In this study, we introduce plant-derived proteins to develop composite biomaterial inks to improve the biocompatibility and mechanical strength of scaffold materials. These proposed composite biomaterial inks are fed into EHDP system for high-precision scaffold fabrication. Two types of composite scaffolds are developed, namely, PCL/zein and PCL/gliadin. With the help of a developed monitoring and identification system, EHDP process parameters and environmental parameters are optimized to fabricate such composite scaffolds. To analyze the scaffolds' performance, mouse embryonic fibroblasts (NIH/3T3) cells were cultured to examine the cellular responses on PCL/zein, PCL/gliadin, and pure

PCL scaffolds. Although the composite inks we discussed are supplied to EHDP system for scaffold building, the application of such inks can also be implemented on several different kinds of 3D printing systems, such as extrusion-based printing and electrospinning.

2. Materials and methods

Natural extracellular matrix (ECM) creates complex physical and chemical environment to support cell/tissue functions. To introduce such complexities to ECM-mimicking fibrous scaffolds, EHDP has been implemented to fabricate scaffolds with aligned fibers to create controllable microstructures using single polymer-based material system. To enhance such EHDP scaffolds' performance, our group has developed plant protein-based composite inks which could distinctly improve fiber surface biocompatibility during cell culture studies.

2.1. Materials

The gliadin power was purchased from Tokyo Chemical Industrial Ltd. (Japan). 3-(4,5-dimethylthiazol-2-yl)-2,5-diphenyltetrazolium bromide (MTT) cytotoxicity assay and CellTiter 96® AQueous One Solution Cell Proliferation Assay were obtained from Abcam Ltd. (China) and Promega Co. Ltd. (USA), respectively. The rest of the chemicals and reagents are similar to those reported previously[23].

2.2. Preparation of PCL/zein and PCL/gliadin biomaterial inks

PCL, PCL/zein, and PCL/gliadin biomaterial inks were prepared for EHDP scaffold fabrication. PCL ink (70 w/v% in glacial acetic acid [AcOH], g/mL) was prepared by dissolving PCL pellets (3.5 g) in acetic acid (5 mL) with stirring for 1 h to allow complete dissolution. Both zein and gliadin are soluble in acetic acid, and we used two weight ratios, that is, 10% w/v and 20% w/v to prepare both PCL/zein and PCL/gliadin inks in this study. Zein or gliadin powder were first dissolved in glacial AcOH to obtain a clear solution. Subsequently, PCL pellets were added to either solution under ultrasonic condition at 50°C and the mixture was stirred 30 min to produce homogenous PCL/gliadin or PCL/zein biomaterial inks.

Two types of PCL/zein biomaterial inks were prepared: PCL/zein-10 (60% w/v PCL, 10% w/v zein in AcOH) and PCL/zein-20 (50% w/v PCL, 20% w/v zein in AcOH). Similarly, two PCL/gliadin biomaterial inks were prepared: PCL/gliadin-10 (60% w/v PCL, 10% w/v gliadin in AcOH) and PCL/gliadin-20 (50% w/v PCL, 20% w/v gliadin in AcOH). The viscosity of zein and gliadin solution (in acetic acid) is low. Thus, the viscosity of such biomaterial inks is mainly determined by the viscosity of PCL solution due to its high concentration, and no significant viscosity difference was observed between these inks.

2.3. EHDP system setup and fabrication process monitoring

Figure 1A shows a schematic diagram of a solution-based EHDP setup, which includes an ink feeding system, a high voltage power supply (0 – 10 kV, Dongwen Co. Ltd., China) and a three-axis precision motorized stage from Aerotech Company (Pittsburgh, PA, USA). The solution feeding system consists of a micro-syringe pump, a disposable syringe (5 mL), a flexible plastic hose, and a stainless steel needle (G20). The voltage output from the high-power supply was applied between the nozzle and the substrate to trigger and maintain EHDP jetting process. The precision stage has a travel range of 150 mm/s with 3 μm accuracy on x and y axes. A polished silicon wafer placed on x-y stage was used as the substrate for fiber deposition. The stage moving speed along x and y directions is set between 100 mm/s and 300 mm/s. The ejected fiber could continuously deposit on the stage with the mechanical drawing force which was generated with the stage moving along x and y axes. As shown in **Figure 1B**, this deposited fiber stacked up gradually and formed a scaffold by following predesigned moving path.

2.4. EHDP fabrication process monitoring

As the EHDP's printing resolution can approach submicron to nanoscale, any slight fluctuations of the environmental factors, such as the variations of temperature, humidity, air flow, and the printing platform vibration due to stage movement, might affect printing accuracy[12]. It also took some time to achieve and maintain a steady flow rate and stage speed, especially for high viscous biopolymer solutions. Besides, corona discharge phenomena are quite common when using PCL/gliadin and PCL/zein inks. This is ascribed to residual charges remained in the peptide chains of gliadin or zein protein, which alters the electrical properties of the composite inks. When the accumulated charges on the droplet surface at the nozzle tip exceeded a critical value, the corona discharge could be observed. If this discharge lasts for a longer time, the EHDP fabrication system can be damaged.

To achieve a reliable fabrication process, it is essential to develop a system to monitor and identify the status of triggered jet and cone. In the developed system, the jet and cone images were recorded using digital microscope (Supereyes B011 digital camera with 1 – 500 magnifications and 30 frames/s) to observe the details of Taylor cone and jet region. To capture images, the camera position, focal length, and shooting angle should be calibrated by comparing the overlapping area of the grayscale nozzle image with a predefined position.

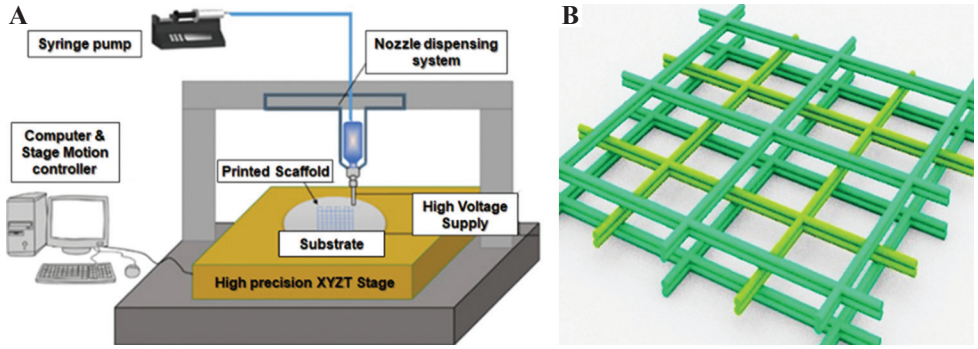

Figure 1. Electrohydrodynamic printing (EHDP) system and scaffold fabrication. (A) Schematic diagram of EHDP system. (B) Scaffold structure by fiber stacking.

To establish a viable manufacturing process and minimize defect-related loss in long time fabrication, the captured EHDP cone and jet images were applied to detect abnormal modes, as shown in **Figure 2A**. The identification task in this EHDP monitoring system involves the application of an image processing algorithm to extract relevant features and a recognition algorithm to determine the modes of Taylor cones. This is very similar to traditional fabrication process monitoring, where feature extraction and selection are applied to determine the input features of machining learning methods for effective condition identification[24,25].

Figure 2B shows a standard cone with a straight jet for EHDP scaffold fabrication. In the EHDP monitoring and identification system, various types of corona discharge were reported. As shown in **Figure 2C**, the corona discharge happened slightly below the needle tip at initial jetting process or during fabrication. Such discharge could be avoided by optimizing EHDP process parameters and environmental parameters. **Figure 2D** shows the current flow through the air from the region surrounding the jet to the grounded substrate. This reduced the surface charge density and increased the jet's lateral stability. Different from the above-mentioned two scenarios, a huge Taylor cone with serious discharge at the needle tip is shown in **Figure 2E**. To avoid possible damages of the EHDP fabrication system, we need to properly vary the biomaterial ink properties, process parameters, and environmental parameters.

Overall, this monitoring and identification system provides intuitive information of EHDP fabrication process and bridges the knowledge gap between the corona discharges and electrical properties of the composite materials. Researchers can evaluate new inks' property and stability during long time printing and gain additional insights into fundamental mechanism causing corona discharges. It can also assist new inks' fabrication process parameter optimization such as applied electric field between the nozzle and the substrate, solution feeding rate, programmed stage speed and moving path, temperature, and humidity.

3. Results and discussion

3.1. Composite scaffold structure and tensile test

The fabricated scaffold fibers with varied material compositions may influence cell-scaffold interactions. To investigate this factor, we prepared scaffolds using the same structural parameters (pore size, fiber diameter, and number of layers), and fabricated PCL, PCL/zein-10, PCL/zein-20, PCL/gliadin-10, and PCL/gliadin-20 scaffolds for comparison.

(1) Composite scaffold structure analysis

The printed scaffolds consist of 12 layers of fibers with a thickness of about 65 – 85 μm. The thickness of PCL, PCL/zein, and PCL/gliadin scaffolds is stated in **Table 1**. The fiber diameter of top layer is approximately 8.9 – 9.4 μm, which is close to typical cell size. Due to the impact of ejected filament onto the previously deposited fiber layers, the fiber diameter of the bottom layers is about twice the diameter of the top layer cross of all scaffolds. The porosity of these scaffolds is about 89 – 92.1%, which is in favor for exchanging nutrition and waste. In **Table 1**, the structural parameters such as fiber diameter, scaffold thickness, bulk density, and porosity are very similar for all the scaffolds. In other words, the proposed biomaterial inks with current components and portion do not influence the morphology of these scaffolds obviously.

As shown in **Figure 3**, PCL and PCL/gliadin scaffolds were observed using a scanning electron microscope (SEM, JSM-6510, JEOL, Japan) for morphology analysis. The pore size was precisely defined, and fibers were precisely stacked in a layer-by-layer manner. For the fabricated scaffolds using PCL/zein and PCL/gliadin inks, there was not much difference in terms of fiber diameter and cross-section structure. In general, these scaffold parameters are independent of the material compositions. The tensile properties of these scaffolds were compared and analyzed in sub-section.

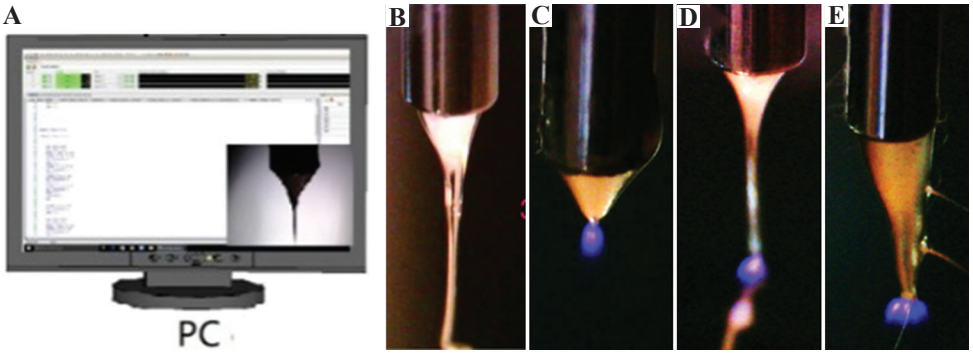

Figure 2. Electrohydrodynamic printing (EHDP) monitoring and discharging phenomena. (A) EHDP monitoring interface. (B) Standard cone. (C) Discharge at initial jet formation. (D) Discharge in fabrication. (E) Huge cone with discharge.

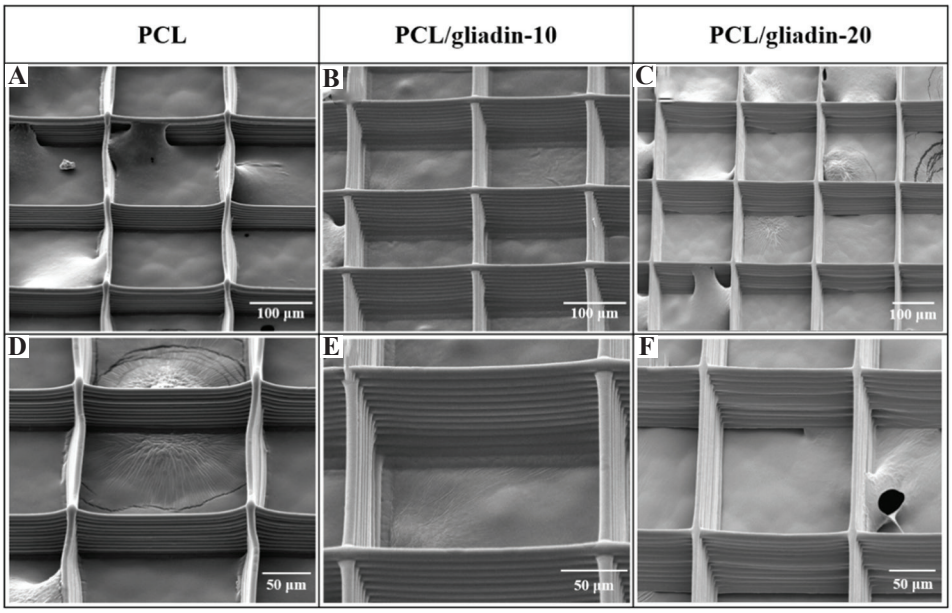

Figure 3. Scanning electron microscope images and their corresponding enlarged views of morphology. (A) and (D) poly(ε-caprolactone) (PCL). (B) and (E) PCL/gliadin-10. (C) and (F) PCL/glaidin-20 scaffolds.

Table 1. Morphological data of printed scaffolds

Scaffolds	PCL	PCL/zein-10	PCL-zein-20	PCL/gliadin-10	PCL/gliadin-20
Fiber diameter (μm)					
Top layer	8.9±1.1	9.0±0.7	9.0±1.1	9.4±0.7	9.1±1.1
Bottom layer	17.4±2.9	18.5±1.0	20.0±2.4	18.1±1.5	17.5v1.7
Thickness (μm)	67.8±7.4	72.4±3.5	77.6±2.4	72.7±2.9	75.2±3.3
Bulk density (kg/ m^3) [1]	1100	1118	1137	1130	1162
Porosity (%)	91.7±0.3	92.1±0.2	91.7±0.5	89.0±0.5	89.6±1.1

[1]Bulk density is estimated based on the densities of PCL, zein, and gliadin in the scaffolds.

(2) Tensile properties of the composite scaffolds

The scaffolds' tensile properties were examined using a universal testing machine (HD-B609B-S, HAIDA, China). The scaffolds were prepared in rectangular shape (4 × 2 cm) and stretched along the longer side. This test was to stretch the scaffolds with an initial gauge length of 20.0 mm at a speed of 1 mm/min and 10 mm/min for pre-loading and loading conditions.

The stress-strain curve of PCL, PCL/gliadin, and PCL/zein scaffolds is illustrated in **Figure 4** and tensile properties of scaffolds are summarized in **Table 2**. In general, PCL scaffold showed a typical amorphous

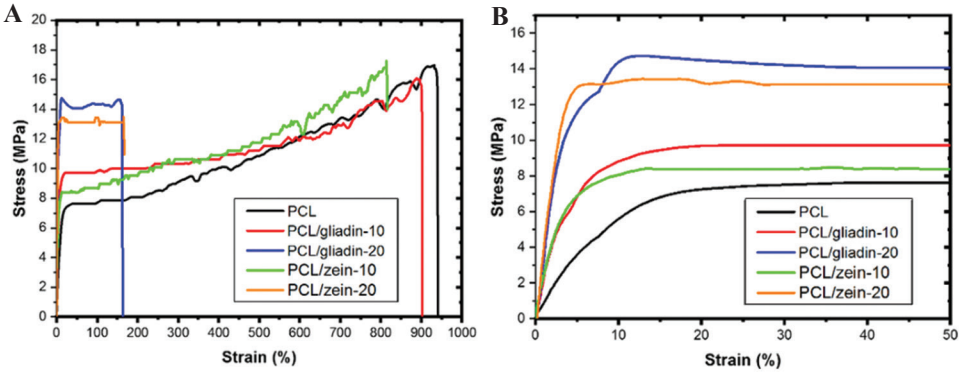

Figure 4. Tensile test of printed scaffolds (A) Stress-strain curve, (B) Enlarged view of initial range.

Table 2. Tensile properties of PCL, PCL/zein, and PCL/gliadin scaffolds

Scaffolds	PCL	PCL/zein-10	PCL/zein-20	PCL/gliadin-10	PCL/gliadin-20
Young's modulus (MPa)	101.3±6.5	241.4±7.9	338.7±38.9	265.3±27.8	465.3±50.9
Yield stress (MPa)	4.5±0.5	6.3±0.3	14.2±0.6	7.2±0.7	15.0±0.6
Yield strain (%)	6.5±0.5	5.4±0.7	6.0±1.0	4.7±0.6	5.4±0.4
Ultimate stress (MPa)	17.1±0.5	15.9±0.5	14.3±0.8	15.7±0.8	14.5±0.7
Ultimate strain (%)	994.4±54.7	802.8±59.1	167.0±50.9	891.2±31.8	120.8±26.0

polymer behavior with three phases, including elastic deformation, yielding, and prolonged strain hardening. The Young's modulus of this PCL scaffold was about 101.3 ± 6.5 MPa, whereas the yield stress and strain were 4.5 ± 0.5 MPa and 6.5 ± 0.5%, respectively. The ultimate stress and strain of the PCL scaffolds were 17.1 ± 1.0 MPa and 994.4 ± 54.7%, which were about 4 and 150 times higher than that at the yield point. These results suggest that PCL is a ductile material with superior roughness because of the reorientation of polymer chains during stretching. When incorporating gliadin nanoparticles into the composite ink, the Young's modulus values of PCL/gliadin-10 and PCL/gliadin-20 scaffolds dramatically increased to 265.3 ± 27.8 MPa and 465.3 ± 50.9 MPa, respectively. The ultimate strain of PCL/gliadin-20 scaffold dropped to 120.8 ± 26.0 MPa, which is only about one-eighth of that of PCL, whereas the ultimate strain of PCL/gliadin-10 scaffolds remained at high level of 891.2 ± 31.8 MPa. The results showed that PCL/gliadin-20 scaffold became stiffer and brittle, while PCL/gliadin-10 scaffold was still ductile with improved hardness. The gliadin nanoparticles could self-assemble into nanosized structures on accounts of the amphiphilic nature of plant proteins in the solution[21]. These nanoparticles form strong intermolecular interactions with PCL polymer chains and increase the mechanical properties of this PCL/gliadin-10 scaffold, that is, Young's modulus and yield stress. This is similar to incorporating inorganic nanoparticles, such as bioactive glass, to improve the mechanical performance of PCL[26]. In addition, the overall elongation is sacrificed when these nanoparticles start to agglomerate at higher concentration and become larger partial continuous phase in some regions.

The tendency of PCL/zein-10 scaffold's stress-strain curve was very similar to that of PCL/gliadin-10 scaffold, since the uniformly dispersed zein nanoparticles in the composite could link the entangled PCL chains through molecular interactions. This strengthening effect increased both Young's modulus and yield stress. Similar to PCL/gliadin-20 scaffold, the toughness of PCL/zein-20 scaffold was sacrificed somehow because of larger portion of zein particles.

Mechanical stimulation is one of the critical elements in the complex microenvironment during cell culture. Since the chemical composition and proportion of composite materials can tune the stiffness, Young's modulus, and strain of the fabricated scaffolds, diverse mechanical stimuli can be created for cell behavior studies. For example, the stiffness of cell local environment can be used to investigate its influence on cellular traction force to regulate cell migration. However, such level of measurement is currently not available in 3D environment.

3.2. Composite scaffolds' cell culture study

Scaffolds' biological studies usually involve the examination of their biocompatibility and biodegradation. The scaffold biodegradation is one of the key factors in tissue regeneration since it provides temporary support for tissue growth and infiltration on implantation and

degrades at a proper rate during tissue regeneration process. This is not a serious issue for cell culture studies since scaffolds are only used for a short time to produce *in vitro* models.

A well-known cell line derived from mouse embryo cells, named NIH/3T3 cell, was cultured on PCL, PCL/gliadin, and PCL/zein scaffolds for biocompatibility evaluation. Due to the concern of side effects from gliadin in cell growth, the cytotoxicity of PCL/gliadin scaffolds was evaluated before cell culture studies.

(1) Cytotoxicity assay of gliadin released from PCL/gliadin scaffolds

The cytotoxicity of the gliadin released from PCL/gliadin scaffolds on NIH/3T3 fibroblast cell was evaluated through colorimetric MTT assay. As shown in **Figure 5A**, the cell viability of NIH/3T3 cells was higher than 95% when incubating together with PCL or PCL/gliadin-10 scaffolds. The cell viability for PCL/gliadin-10 scaffolds was slightly higher than that of the control group (cell culture in medium), while this value was only about 85% for PCL/gliadin-20 scaffolds. This suppressive effect was caused increased release of gliadin from the PCL/gliadin-20 scaffold since its corresponding weight loss in 72 h was obviously bigger than that of PCL/gliadin-10.

The weight loss of PCL/gliadin scaffolds was measured by immersing them in phosphate-buffered saline (PBS, 10 mM, pH 7.4) with the addition of 1% antibiotics at an incubator (37°C). As in **Figure 5B**, the weight loss of PCL scaffold versus time was negligible, while the weight loss for PCL/gliadin-10 and PCL/gliadin-20 scaffolds was up to 14.5% and 21.2%, respectively, in 120 h. Nearly 90% of the total weight loss happened in the first 20 h. Meanwhile, the release of gliadin did not change the pH value of the solution as gliadin is neutral substance in the solution.

(2) Cell viability and proliferation studies in the PCL/gliadin scaffolds

The cellular interactions of these fabricated PCL/gliadin scaffolds were further studied in this sub-section. The influence of gliadin component was investigated by directly culturing NIH/3T3 cells on the PCL/gliadin scaffolds. The scaffolds were cut into unified round specimens and inserted in the ultralow attachment culture plate. A small volume of cell suspension was directly pipetted onto the specimen in each well for cell seeding. After incubation for few hours, the culture medium was added, and some cells adhered onto the scaffold fibers.

Cell seeded scaffolds were visualized by confocal laser scanning microscopy (CLSM, LSM-880, ZEISS, Germany). After fixation in paraformaldehyde, the cell nuclei and membrane were stained with Hoechst 33342 and DiI dye, which emit blue and red fluorescence, respectively, on laser excitation. **Figure 6A** shows the CLSM images of cell cultured on PCL and PCL/gliadin scaffolds on days 1, 3, 7, and 14. On day 1, the spheroid cells could partially attach onto the scaffolds. After 3 days, most of the attached cells started to spread, orient, elongate along the fiber directions, and extend the filopodia at leading edge to grab on the adjacent fibers. This resembles fibroblast migration *in vivo* with front-end/back-end polarity[27]. The cell adhesion and proliferation were not homogeneous on the first few days because of uneven cell distribution during initial cell seeding. From day 3 to day 7, the fibroblasts actively proliferated from the scaffold's side walls to the center of pores, formed a unique circular structure, and eventually merged to form a cellular film. Finally, a film-like cell sheet was observed in each cultured scaffold on day 14.

A colorimetric cell proliferation assay (CellTiter 96® AQueous One Solution) was applied to count cell numbers. In cell culture experiments, the ultra-low attachment culture plate (Corning 3473) was used for

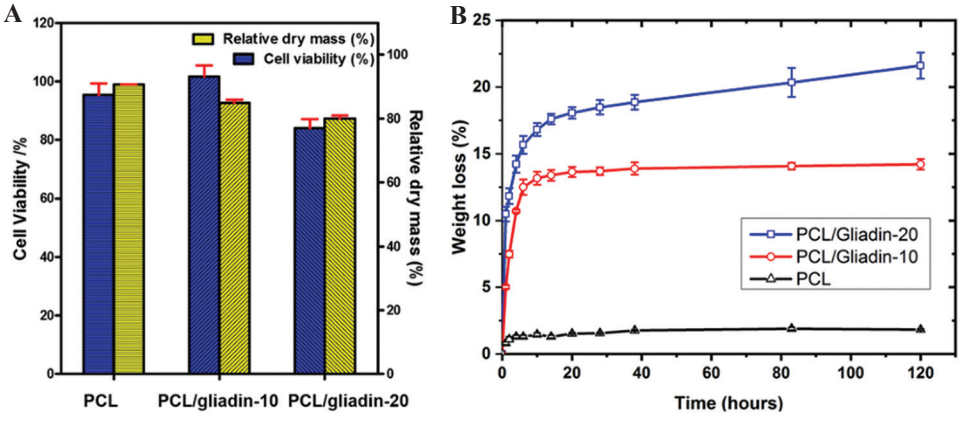

Figure 5. *In vitro* cytotoxicity test (A) Cell viability and relative dry mass loss after seeding cells on poly(ε-caprolactone) (PCL) and PCL/gliadin scaffolds for 72 h; (B) weight loss profile of PCL and PCL/gliadin scaffolds in phosphate-buffered saline.

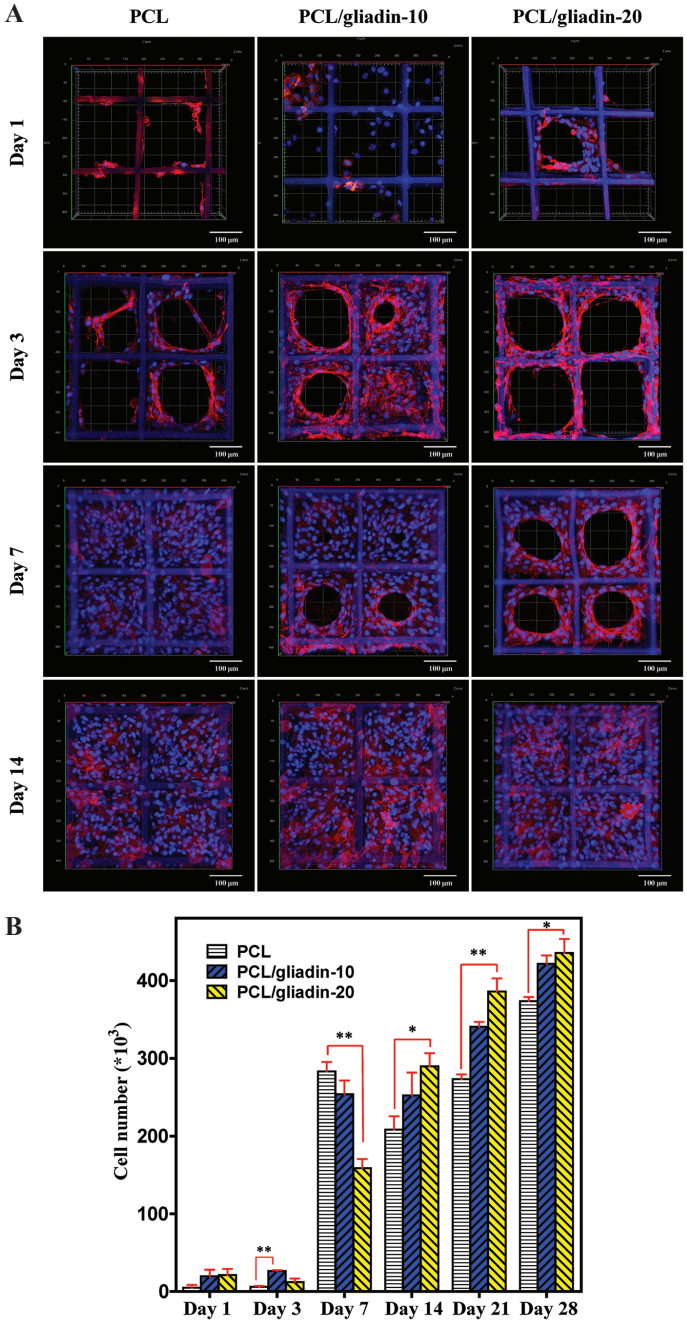

Figure 6. 3D cell culture study on gliadin containing scaffolds (A) Confocal laser scanning microscopy images of NIH/3T3 cell cultured on poly(ε-caprolactone) (PCL) and PCL/gliadin scaffolds. (B) NIH/3T3 cell numbers on PCL and PCL/gliadin scaffolds by CellTiter 96® AQueous One Solution assay ($n = 5$, $^*P < 0.05$, $^{**}P < 0.01$).

cell seeding. For this kind of culture plate, cells were unable to attach onto the bottom substrate. They either adhered onto the scaffold fibers or gathered to form cell spheroids that floated in the medium. Before performing cell counts, the cell seeded scaffolds were washed with PBS thrice to get rid of unattached cells and transferred to a new plate for a colorimetric cell counting assay. Thus, only the cells that attached onto the scaffold were counted for the comparison of cell numbers.

As illustrated in **Figure 6B**, the number of cell attached to the gliadin-containing scaffolds was approximately 4 times higher than that of the PCL scaffolds on day 1. This might be attributed to the improved hydrophilicity of the fiber surface, and certain amino acid residues of gliadin might act as anchor points for cell recognition and binding. On day 3, the cells adapted to the microenvironment and the number of cells that attached to the PCL and PCL/gliadin-10

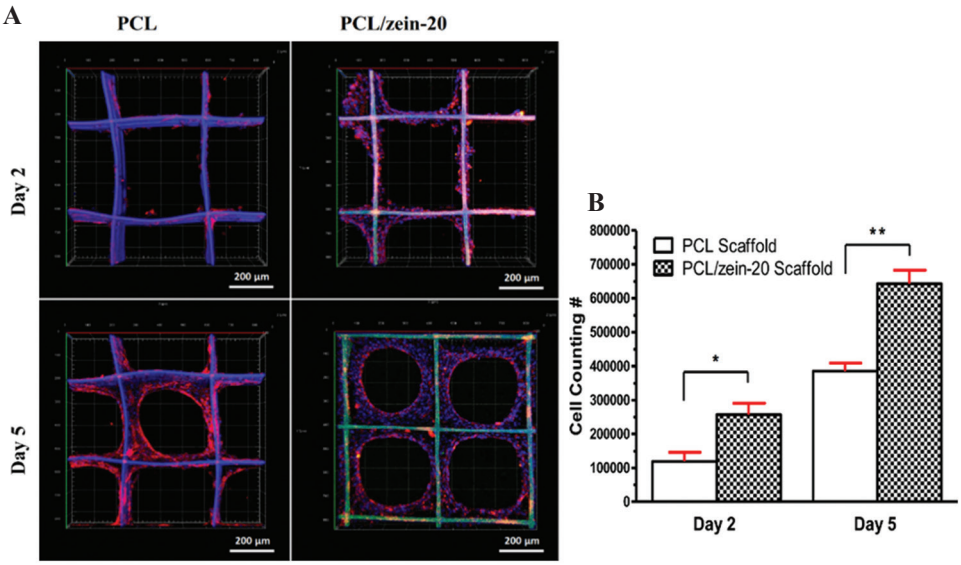

Figure 7. 3D cell culture study on zein containing scaffolds (A) Confocal laser scanning microscopy images of NIH/3T3 cell culture on poly(ε-caprolactone) (PCL) and PCL/zein-20 scaffolds. (B) NIH/3T3 cell number on PCL and PCL/zein-20 scaffolds.(n = 3, $*P < 0.05$, $**P < 0.01$). (Reproduced from Ref. Jing *et al*.[23] with permission).

scaffolds slightly increased. However, the cell number on the PCL/gliadin-20 scaffolds declined by around 40%, which is consistent with the results of cytotoxicity assay in **Figure 5.** This growth inhibition effect is caused by increased release of gliadin component. From day 7 to day 28, the cell number continued to increase, and the biggest increase was observed from the PCL/gliadin-20 scaffolds. This is attributed to the larger number of nano-pores and cracks created by the released gliadin which facilitate cell migration, proliferation, and infiltration.

In general, the gliadin-containing scaffolds can promote cell adhesion of NIH/3T3 cells. It can facilitate cell proliferation more effectively than PCL for relatively long-term cell culture until week 4. The inhibition effect from PCL/gliadin-20 scaffold only shows at the earlier stage.

(3) Cell viability and proliferation studies in PCL/zein scaffolds

Zein is almost insoluble in water or PBS solution; therefore, the evaluation of weight loss of PCL/gliadin in cell culture was not applicable for PCL/zein scaffolds. Since no cytotoxicity of zein has been reported in previous studies[23], we evaluated biological performance of fabricated PCL/zein scaffolds directly. **Figure 7A** shows the CLSM images of seeding NIH/3T3 cells on PCL and PCL/zein-20 scaffolds on different days and **Figure 7B** shows the corresponding cell counting results. On day 2, NIH/3T3 cells were inclined to adhere onto the side surface of these scaffolds and the number of cells on the PCL/zein-20 scaffold was about twice of that on the PCL scaffolds. The cell affinity increased with zein portion in the scaffolds. On day 5, NIH/3T3 cells distributed homogeneously within the scaffolds and formed circular cell clusters. Eventually, cellular films could be observed within the scaffold pores. Seemingly, zein-containing fiber surface was more suitable for cell recognition and adhesion due to the functional groups from the amino acid side chains. The cell affinity toward scaffold could be adjusted by varying weight percentage of zein in the composite inks.

(4) Plant protein nanoparticles in cell culture applications

Plant protein nanoparticles affect scaffolds' cell culture applications through protein particle signaling, surface morphology change, and scaffold degradation after the release of nanoparticles. Fibrous scaffold composition has a profound influence on cell behavior such as signaling and contact guidance[1]. This inspires novel strategies to manipulate fiber surface with chemical stimuli for enhanced cell attachment and proliferation. The composite scaffolds containing plant protein can benefit cell culture process in two steps. First, the fiber-containing protein nanoparticles favor cell attachment and colonization. As the key factor to improve scaffolds' cell affinity at the initial stage, this effect can be modulated by regulating the density, size, and dimensional scale of nanoparticles. With the increasing applications of plant protein nanoparticles in developing composite biomaterial inks, intriguing ECM-mimicking fibrous scaffolds can be created with improved cell–scaffold interface.

Both zein and gliadin particles are prone to self-assemble to nanospheres in biomaterial inks because

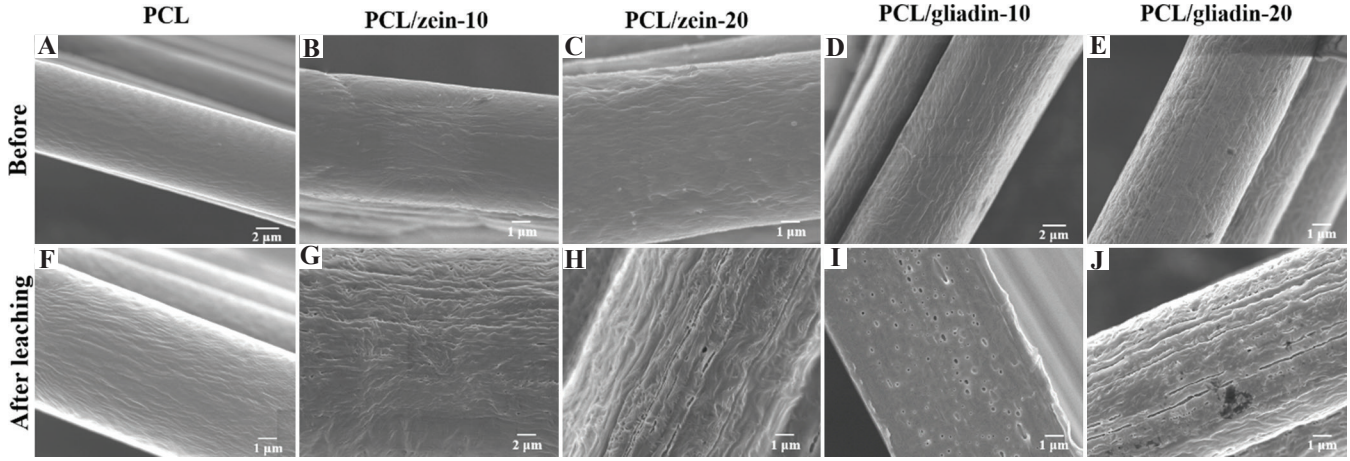

Figure 8. Fiber surface morphological changes of before and after the leaching treatment for 48 h. (A) and (F) poly(ε-caprolactone) (PCL). (B) and (G) PCL/zein-10. (C) and (H) PCL/zein-20. (D) and (I) PCL/gliadin-10. (E) and (J) PCL/gliadin-20. PCL/gliadin and PCL/zein scaffolds were leached in culture media and 70% ethanol, respectively. (PCL scaffold was used as control).

of their amphiphilicity[17]. It is difficult to compare the cellular behaviors of zein and gliadin on PCL/zein and PCL/gliadin scaffolds in the same way, as gliadin can quickly dissolve in the culture medium but zein has poor water solubility. Hence, leaching treatment was applied to simulate the surface morphology change of scaffolds *in vitro*. Before the leaching treatment, the PCL, PCL/zein, and PCL/gliadin scaffolds were dried *in vacuo* at 40°C until they reached a constant weight. Then, the scaffolds were completely immersed in 70% ethanol with shaking (80 rpm) for 48 h. The solution was replenished every 12 h. After treatment, the scaffolds were washed with deionized water thrice and then dried *in vacuo* until they reached a constant weight. Using this method, nanoparticles on the composite scaffold fiber surface were released into the culture medium, and nanopores and cracks were generated.

According to **Figure 8A-E**, surface morphology of fibers was almost the same for all the scaffold materials because relatively small portion of nanoparticles in the composite ink materials was not sufficient to engender noticeable changes. As shown in **Figure 8A and 8F**, no obvious change was found on PCL scaffold fiber surface before and after the leaching treatment since PCL cannot dissolve in ethanol. The size and density of gliadin and zein particles could be speculated from the surface morphology change of fibers, as shown in **Figure 8G-J**, through leaching. Based on the voids on the fiber surface (**Figure 8G-8J**), it can be speculated that both zein and gliadin can self-assemble into nanoparticles in the composite ink, which can influence mechanical properties of printed scaffolds. Moreover, higher density of nanopores and cracks could be observed on PCL/zein-20 and PCL/gliadin-20 scaffolds compared with those observed on PCL/zein-10 and PCL/gliadin-10 scaffolds. The scale of such nanopores was also larger for the PCL/zein-20 and PCL/gliadin-20 scaffolds, which is due to the increasing portion and size of plant protein particles in the composite inks. For example, the average pore size of nanopores on **Figure 8I and 8J** is 133.1 ± 47.4 nm and 209.2 ± 76.2 nm, respectively. These holes and fissures interconnected with each other, generated a highly cavernous structure, and increased surface area exponentially; all of which significantly facilitated cell migration, proliferation, and infiltration.

In general, the developed composite scaffolds degrade in two interrelated processes. First, zein and gliadin particles can be released from scaffold fiber surface under physiological environment, but in different ways. Since gliadin is a water-soluble protein, its particles from PCL/gliadin scaffolds can be dissolved in PBS solution. For PCL/zein scaffolds, various proteases can hydrolyze zein into peptides or amino acids. Thus, nanopores and cracks on the fiber surface can be observed on both PCL/zein and PCL/gliadin scaffolds. Second, such nanoporous surface can accelerate the composite scaffolds' degradation, since PCL polymer chains might be synchronously released into solution when zein or gliadin domain in the composite is degraded as a result of molecular level blending. Thus, the degradation rate of the composite scaffolds can be controlled by adjusting the mixing ratio of plant protein and PCL in the biomaterial ink. In general, the composite material scaffolds degrade faster than the pure PCL scaffolds with the same scaffold structural parameters.

Plant proteins have been used to develop composite scaffolds for several reasons, including their biocompatibility, biodegradability, safety, low cost, processibility, and ductility[28]. Nevertheless, the possible immunogenicity effects restrict their biomedical applications. Of course, whether the occurrence of immune response depends on the dose of plant protein

within the scaffolds still requires further and thorough investigations. The availability of a few synthetic biopolymers and plant proteins for developing composite materials has given us the opportunity to try out different permutations in an attempt to fine-tube mechanical properties and biological performance of the scaffolds. The purity level of these plant proteins may also affect their physicochemical properties and act as a limiting factor in their wide usage. More researches are scaling up the current protein extraction and purifying techniques and clinical trials on more composite scaffolds are expected soon.

4. Conclusion

Plant proteins, such as zein and gliadin, have been reported to play a critical role in regulating cell behaviors. Their interaction that occurs at nanoscale has not been comprehensively discussed in the context of fibrous scaffolds. Because of the unique advantages of such plant proteins, we explore the possibilities of utilizing them as scaffold materials for cell culture applications. Two types of plant protein-based composite inks, called the PCL/gliadin and PCL/zein, were prepared. The corresponding scaffolds were fabricated using EHDP technology. A monitoring and identification system was developed to optimize the corresponding scaffold fabrication process. Both PCL/gliadin-10 and PCL/zein-10 scaffolds have enhanced tensile strength and cell viability in terms of cell affinity and proliferation. Compared with PCL scaffold, the PCL/gliadin-20 and PCL/zein-20 scaffolds are brittle and stiffer. Moreover, the proportion of plant proteins can be altered to control the tensile strength and cell viability of these composite scaffolds. Thus, the composite materials, PCL/gliadin-10 and PCL/zein-10, are recommended for tissue engineering as they can not only improve scaffolds' mechanical strength to support cell growth but also exhibit favorable biocompatibility for cell culture applications. The developed composite scaffolds may provide valuable *in vitro* platform to study cell biology in 3D microenvironment. With the increasing applications of plant protein nanoparticles in developing new composite biomaterial inks, intriguing ECM-mimicking fibrous scaffolds can be created with improved cell–scaffold interface, which can be used to culture diverse cells and form organoids.

Acknowledgments

This work is financially supported by the Key Program Special Fund in Xi'an Jiaotong-Liverpool University (XJTLU) under Grant KSF-A-09 and KSF-E-37.

Conflict of interest

The authors declare no conflicts of interest.

Author contribution

L.J., H.L., and X.W. designed the overall experimental plan and performed experiments. L.J. interpreted data and wrote the manuscript with support from J.S. and H.L. J.S. and D.H. supervised the project and conceived the original idea. All authors read and approved the manuscript.

References

1. Hutmacher DW, 2001, Scaffold Design and Fabrication Technologies for Engineering Tissues State of the Art and Future Perspectives. *J Biomater Sci Polym Ed*, 12:107–24. http://doi.org/10.1163/156856201744489.
2. Pampaloni F, Reynaud EG, Stelzer EH, 2007, The Third Dimension Bridges the Gap between Cell Culture and Live Tissue. *Nat Rev Mol Cell Biol*, 8:839–45. http://doi.org/10.1038/nrm2236.
3. Walpita D, Hay E, 2002, Studying Actin-dependent Processes in Tissue Culture. *Nat Rev Mol Cell Biol*, 3:137–41. http://doi.org/10.1038/nrm727.
4. Gudjonsson T, Rønnov-Jessen L, Villadsen R, *et al.*, 2002, Normal and Tumor-derived Myoepithelial Cells Differ in their Ability to Interact with Luminal Breast Epithelial Cells for Polarity and Basement Membrane Deposition. *J Cell Sci*, 115:39.
5. Dhiman HK, Ray AR, Panda AK, 2005, Three-dimensional Chitosan Scaffold-based MCF-7 Cell Culture for the Determination of the Cytotoxicity of Tamoxifen. *Biomaterials*, 26:979–86. http://doi.org/10.1016/j.biomaterials.2004.04.012.
6. Baker BM, Chen CS, 2012, Deconstructing the Third Dimension-how 3D Culture Microenvironments Alter Cellular Cues. *J Cell Sci*, 125:3015–24. http://doi.org/10.1242/jcs.079509.
7. Ma PX, 2004, Scaffolds for Tissue Fabrication. *Mater Today*, 7:30–40.
8. Chia HN, Wu BM, 2015, Recent Advances in 3D Printing of Biomaterials. *J Biol Eng*, 9:4.
9. Ozbolat IT, Hospodiuk M, 2016, Current Advances and Future Perspectives in Extrusion-Based Bioprinting. *Biomaterials*, 76:321–43. http://doi.org/10.1016/j.biomaterials.2015.10.076.
10. Ng WL, Lee JM, Zhou M, *et al.*, 2020, Vat Polymerization-based Bioprinting-Process, Materials, Applications and Regulatory Challenges. *Biofabrication*, 12:022001. http://doi.org/10.1088/1758-5090/ab6034.
11. Onses MS, Sutanto E, Ferreira PM, *et al.*, 2015, Mechanisms, Capabilities, and Applications of High-Resolution

Electrohydrodynamic Jet Printing. *Small*, 11:4237–66. http://doi.org/10.1002/smll.201500593.

12. Liu H, Vijayavenkataraman S, Wang D, *et al.*, 2017, Influence of Electrohydrodynamic Jetting Parameters on the Morphology of PCL Scaffolds. *Int J Bioprint*, 3:72–82. http://doi.org/10.18063/ijb.2017.01.009.
13. Guvendiren M, Molde J, Soares RMD, *et al.*, 2016, Designing Biomaterials for 3D Printing. *ACS Biomater Sci Eng*, 2:1679–93. http://doi.org/10.1021/acsbiomaterials.6b00121.
14. Sun J, Vijayavenkataraman S, Liu H, 2017, An Overview of Scaffold Design and Fabrication Technology for Engineered Knee Meniscus. *Materials* (*Basel*), 10:29. http://doi.org/10.3390/ma10010029.
15. Woodruff MA, Hutmacher DW, 2010, The Return of a Forgotten Polymer Polycaprolactone in the 21st Century. *Prog Polym Sci*, 35:1217–56. http://doi.org/10.1016/j.progpolymsci.2010.04.002.
16. Lam CX, Hutmacher DW, Schantz JT, *et al.*, 2009, Evaluation of Polycaprolactone Scaffold Degradation for 6 Months *In Vitro* and *In Vivo*. *J Biomed Mater Res A*, 90:906–19.
17. Wan ZL, Guo J, Yang XQ, 2015, Plant Protein-based Delivery Systems for Bioactive Ingredients in Foods. *Food Funct*, 6:2876–89. http://doi.org/10.1039/c5fo00050e.
18. Anderson TJ, Lamsal BP, 2011, REVIEW: Zein Extraction from Corn, Corn Products, and Coproducts and Modifications for Various Applications: A Review. *Cereal Chem J*, 88:159–73. http://doi.org/10.1094/cchem-06-10-0091.
19. Paliwal R, Palakurthi S, 2014, Zein in Controlled Drug Delivery and Tissue Engineering. *J Control Release*, 189:108–22. http://doi.org/10.1016/j.jconrel.2014.06.036.
20. He M, Jiang H, Wang R, *et al.*, 2017, Fabrication of Metronidazole Loaded Poly (ε-Caprolactone)/Zein Core/Shell Nanofiber Membranes Via Coaxial Electrospinning for Guided Tissue Regeneration. *J Colloid Interface Sci*, 490:270–8. http://doi.org/10.1016/j.jcis.2016.11.062.
21. Urade R, Sato N, Sugiyama M, 2018, Gliadins from Wheat Grain: An Overview, from Primary Structure to Nanostructures of Aggregates. *Biophys Rev*, 10:435–43. http://doi.org/10.1007/s12551-017-0367-2.
22. Koning F, 2015, Adverse Effects of Wheat Gluten. *Ann Nutr Metab*, 67 Suppl 2:8–14.
23. Jing L, Wang X, Liu H, *et al.*, 2018, Zein Increases the Cytoaffinity and Biodegradability of Scaffolds 3D-Printed with Zein and Poly(epsilon-caprolactone) Composite Ink. *ACS Appl Mater Interfaces*, 10:18551–9. http://doi.org/10.1021/acsami.8b04344.s001.
24. Sun J, Hong GS, Rahman M, *et al.*, 2005, Improved Performance Evaluation of Tool Condition Identification by Manufacturing Loss Consideration. *Int J Prod Res*, 43:1185–204.
25. Jie S, Hong GS, Rahman M, *et al.*, 2002, Feature Extraction and Selection in Tool Condition Monitoring System. In: Australian Joint Conference on Artificial Intelligence, Springer, Berlin, Germany, pp. 487-497. http://doi.org/10.1007/3-540-36187-1_43.
26. Castro AG, Diba M, Kersten M, *et al.*, 2018, Development of a PCL-silica Nanoparticles Composite Membrane for Guided Bone Regeneration. *Mater Sci Eng C Mater Biol Appl*, 85:154–61.
27. Meshel AS, Wei Q, Adelstein RS, *et al.*, 2005, Basic Mechanism of Three-dimensional Collagen Fibre Transport by Fibroblasts. *Nat Cell Biol*, 7:157–64. http://doi.org/10.1038/ncb1216.
28. Reddy N, Yang Y, 2011, Potential of Plant Proteins for Medical Applications. *Trends Biotechnol*, 29:490–8.